

## Self-Assembling Peptidomimetic Monolayer Nucleates Oriented CdS Nanocrystals

Haimanot Bekele,<sup>†</sup> Janos H. Fendler,<sup>‡</sup> and Jeffery W. Kelly<sup>\*,†</sup>

Department of Chemistry and the Skaggs Institute of  
Chemical Biology, The Scripps Research Institute  
10550 North Torrey Pines Road MB 12  
La Jolla, California 92037  
Center for Advanced Materials Processing  
Clarkson University, P.O. Box 5814  
Potsdam, New York 13699-5814

Received April 30, 1999

Appropriate organic matrices can control the size, shape, and morphology of inorganic crystals, leading to functional composite materials. The inorganic crystals composing biominerals are precisely orchestrated<sup>1</sup> by the organic matrix; this kind of control is desired in synthetic composite materials. Recent reports outline the successful syntheses of bio-inspired materials.<sup>2</sup> Herein, we introduce a peptidomimetic matrix that folds and self-assembles into a two-dimensional (2D)  $\beta$ -sheet monolayer at an air–water interface, nucleating the {01.0} face of CdS nanocrystals. The enhanced properties of nanocrystals have led to several reports focused on the control of particle size via organic templates;<sup>2c,3–5</sup> however, none of these involve peptidomimetic monolayers that can be designed and easily synthesized.

Amphiphilic peptidomimetics **A** and **B** (Figure 1) contain a 4-(2'-aminoethyl)-6-dibenzofuranpropanoic acid residue (**1**) which nucleates  $\beta$ -hairpin folding.<sup>6a</sup> These hairpins typically self-assemble into  $\beta$ -sheet fibrils.<sup>6b</sup> Incorporation of hydrophobic  $\alpha$ -amino acid residues such as *N*-butyl glutamide at every other position allows peptidomimetics **A** and **B** to dissolve in CHCl<sub>3</sub>/HFIP and self-assemble into a 2D  $\beta$ -sheet monolayer at an air–water interface, with the hydrophilic side chains projecting into the H<sub>2</sub>O.<sup>6c</sup> The hydrophilic surfaces of the amphiphilic peptidomimetic **A** (acidic) and **B** (basic) monolayers differ, allowing an evaluation of the functional group requirements for CdS nanocrystalline growth.

Peptidomimetic monolayers were characterized by a Langmuir–Blodgett trough and spectroscopy (Figure 2).<sup>7</sup> The pepti-

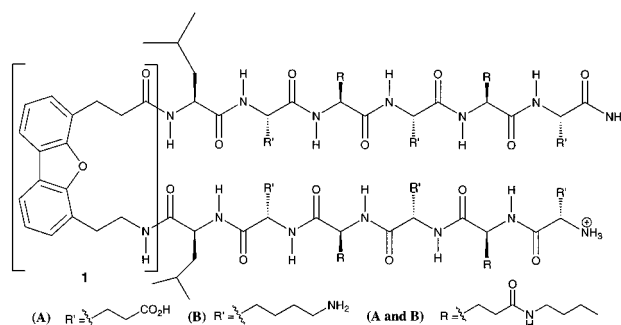


Figure 1. Primary structure of peptidomimetics **A** and **B**.

domimetics appear to fold into a  $\beta$ -hairpin that self-assembles into a stable monolayer on a 10 mM CdCl<sub>2</sub> aqueous subphase (265 Å<sup>2</sup>/molecule) as discerned from pressure–area isotherms. The FT-IR amide I band at 1620 cm<sup>-1</sup> and the far-UV CD minimum at 215 nm are characteristics of assembled  $\beta$ -sheet structures.<sup>8</sup>

Transmission electron microscopy (TEM), atomic force microscopy (AFM), and optical spectroscopy revealed differences in CdS crystal size and orientation for crystallites nucleated on peptidomimetic **A**, relative to those formed in solution or on peptidomimetic **B**. Peptidomimetic **A** spontaneously forms a monolayer in a recrystallization dish by self-assembly and nucleates CdS crystal growth, limiting the crystals to ~25–50 Å in width and length, Figure 3.<sup>9</sup> Electron diffraction studies of the CdS crystallites nucleated on peptidomimetic **A** confirm that they represent the wurtzite lattice structure (Figure 3a), as discerned by the ring patterns corresponding to {10.1}, {10.3}, {20.2}, {20.4}, and {20.5} reflections. All crystallites had their {120} axis normal to the peptidomimetic monolayer, implying that growth occurred from the {01.0} basal plane. HR-TEM studies of the CdS crystallites show patches of lattice fringes that are ~27–54 Å in diameter (70% in the 36–45 Å range) with an experimental *d* spacing of 3.26 Å, closely representing the *d* spacing of the {10.1} planes in CdS, Figure 3b. The CdS crystals are all oriented roughly in the same direction on the monolayer, strongly suggesting long-range order in the peptidomimetic **A** monolayer. AFM studies demonstrate that the CdS crystals on peptidomimetic **A** are 80 Å in height and small in size (~25–50 Å), consistent with the TEM data. CdS crystals formed at the air–aqueous interface in the absence of peptidomimetic (up to 2 mm in diameter) or those nucleated with the basic peptidomimetic **B** monolayer (>60 Å in diameter) were heterogeneous in size, nonoriented, and too thick to be analyzed confidently by AFM.

Consideration of the peptidomimetic monolayer organization and the {01.0} plane of the CdS crystals suggests a lattice match and epitaxial growth (Figure 4) that may explain the approximate 27–54 Å size of the nanocrystals. While complete assessment of the packing of the peptidomimetic monolayer is difficult, we have demonstrated that it adopts an intermolecular  $\beta$ -sheet structure at the surface (Figure 2), implying a 4.75 Å average  $\beta$ -strand-strand separation and a 6.9 Å distance separating alternating C<sub>α</sub> atoms in each  $\beta$ -strand. A model for our peptido-

(8) (a) Woody, R. W. In *Circular Dichroism and Conformational Analysis of Biomolecules*; Fasman, G. D., Ed.; Plenum Press: New York, 1996; pp 25–67. (b) Torii, H.; Tasumi, M. In *Infrared Spectroscopy of Biomolecules*; Mantsch, H. H., Chapman, D., Eds.; John Wiley & Sons: New York, 1996; pp 1–18.

(9) A 40% excess of peptidomimetic in solution<sup>7</sup> was spread on a clean 1 × 10<sup>-2</sup> M CdCl<sub>2</sub> subphase to give a coverage of 265 Å<sup>2</sup>/molecule (~200 Å<sup>2</sup> molecule from modeling) in a circular trough. H<sub>2</sub>S gas in a 3 cm<sup>3</sup> syringe equipped with a needle was placed above the monolayer to diffuse and initiate mineralization. CdS particles were transferred by the horizontal lifting technique to a carbon coated 200-mesh copper grid (TEM) or a mica substrate (AFM).

<sup>†</sup> The Scripps Research Institute.

<sup>‡</sup> Clarkson University.

(1) Weiner, S. *CRC Crit. Rev. Biochem.* **1986**, *20*, 365–408.

(2) (a) Addadi, L.; Weiner, S. *Angew. Chem., Int. Ed. Engl.* **1992**, *31*, 153–169. (b) Berman, A.; Ahn, D. J.; Lio, A.; Salmemon, M.; Reichert, A.; Charych, D. *Science* **1995**, *269*, 515–518. (c) Fendler, J. H.; Meldrum, F. C. *Adv. Mater.* **1995**, *7*, 607–629. (d) Laursen, R. A.; DeOliveira, D. B. *J. Am. Chem. Soc.* **1997**, *119*, 10627–10631. (e) Mann, S.; Archibald, D. D.; Didymus, J. M.; Douglas, T.; Heywood, B. R.; Meldrum, F. C.; Reeves, N. *Science* **1993**, *261*, 1286–1292. (f) Falini, G.; Albeck, S.; Weiner, S.; Addadi, L. *Science* **1996**, *271*, 67–69. (g) Majewski, J.; Popovitz-Biro, R.; Kajaer, K.; Als-Nielsen, J.; Lahav, M.; Leiserowitz, L. *J. Phys. Chem.* **1994**, *98*, 4087–93. (h) Belcher, A. M.; Wu, X. H.; Christensen, R. J.; Hansma, P. K.; Morse, D. E. *Nature* **1996**, *381*, 56–58.

(3) (a) Colvin, V. L.; Schlamp, M. C.; Alivisatos, A. P. *Nature* **1994**, *370*, 354–357. (b) Nirmal, M.; Dabbousi, B. O.; Bawendi, M. G.; Macklin, J. J.; Trautman, J. K.; Harris, T. D.; Brus, L. E. *Science* **1996**, *383*, 802–804.

(4) (a) Youn, H. C.; Baral, S.; Fendler, J. H. *J. Phys. Chem.* **1988**, *92*, 6320–6327. (b) Meldrum, F. C.; Wade, V. J.; Nimmo, D. L.; Heywood, B. R.; Mann, S. *Nature* **1991**, *349*, 684–687.

(5) Dameron, C. T.; Reese, R. N.; Mehra, R. K.; Kortan, A. R.; Carrol, P. J.; Steigerwald, M. L.; Brus, L. E.; Winge, D. R. *Nature* **1989**, *338*, 596–597.

(6) (a) Tsang, K. Y.; Diaz, H.; Graciani, N.; Kelly, J. W. *J. Am. Chem. Soc.* **1994**, *116*, 3988–4005. (b) Choo, D.; Schneider, J. P.; Graciani, N. R.; Kelly, J. W. *Macromolecules* **1996**, *29*, 355–366. (c) See Figure 4a.

(7) A known concentration of peptidomimetic dissolved in HFIP ( $\epsilon = 17797$  L mol<sup>-1</sup> cm<sup>-1</sup>,  $\lambda = 282$ ) was used to make a 4 × 10<sup>-3</sup> M solution in CHCl<sub>3</sub>:HFIP (9:1) employed for monolayer formation on an aqueous subphase (1 × 10<sup>-2</sup> M CdCl<sub>2</sub>). Monolayers were transferred to either a CaF<sub>2</sub> or quartz substrate by the vertical lifting technique.

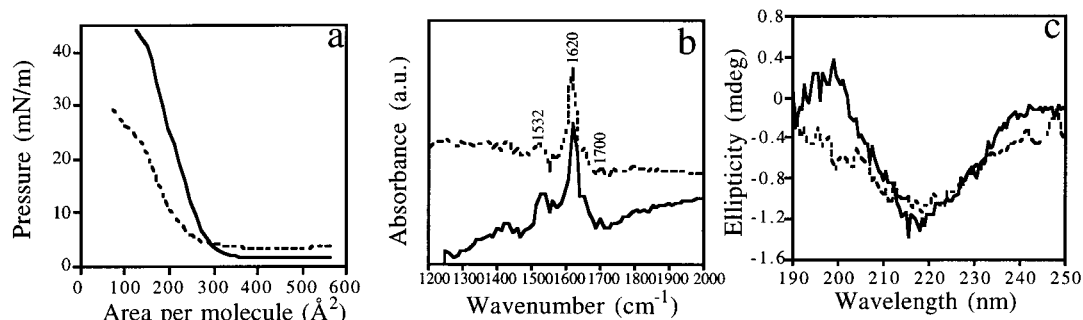


**Figure 2.** (a) Pressure–area isotherm of peptidomimetics **A** (—) and **B** (---) on a  $1 \times 10^{-2}$  M  $\text{CdCl}_2$  subphase. (b) Transmission FT-IR spectra of peptidomimetic monolayers **A** (—) and **B** (---) on  $\text{CaF}_2$ . (c) Far-UV CD spectra of peptidomimetic monolayers **A** (—) and **B** (---) on quartz.

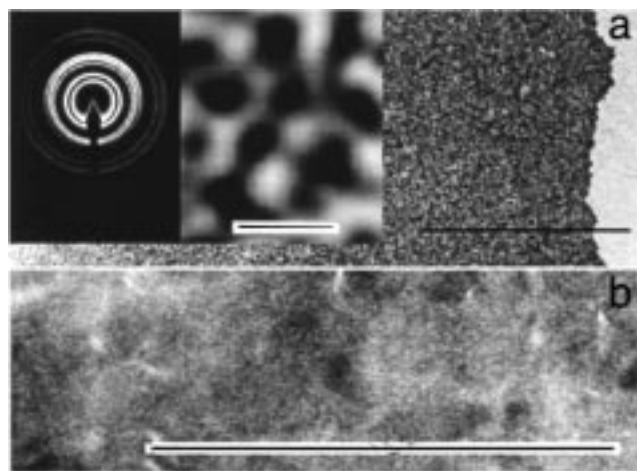


**Figure 3.** (a) Transmission electron micrograph of CdS nanocrystals on a peptidomimetic **A** monolayer (scale bar is 500 nm). The right inset is a magnified view showing dispersed particles that are largely uniform in diameter (scale bar is 15 nm). The left inset represents the electron diffraction (ED) pattern of CdS particle on monolayer **A**. (b) High-resolution TEM image of the nucleated CdS nanocrystal showing the lattice fringes (scale bar is 40 nm).

mimetic is shown in Figure 4a, representing a side view where the hydrophilic (e.g., Glu) and hydrophobic side chains are shown in red and green, respectively. For the  $\{01.0\}$  nucleation face (Figure 4b) there is a good match between the Cd–Cd distance of 6.72 Å in the  $\langle 001 \rangle$  direction and the glutamic acid  $\text{C}_\alpha$ – $\text{C}_\alpha$  atom separation distance of 6.9 Å ( $\sim 3\%$  mismatch) within a single  $\beta$ -strand. An explanation for the size control observed in the  $\langle 001 \rangle$  (c) direction comes from the 14 Å separation between the proximal glutamic acid residues on successive head-to-tail assembled peptidomimetic molecules (Figure 4a). A 14 Å separation is much greater than the 6.72 Å separation required for lattice match; hence, crystal growth in the  $\langle 001 \rangle$  direction appears to be controlled by strand length. The Cd layers in the “b” direction are staggered by 3.36 Å; hence, the projection of the crystal in the  $\langle 001 \rangle$  direction is  $\sim 20$  Å in length, the minimum crystal length observed by TEM.

Lattice match in the  $\langle 100 \rangle$  CdS (a) direction is less optimal with a 4.14 Å Cd–Cd distance and a 4.75 Å  $\beta$ -strand–strand separation ( $\sim 13\%$  mismatch). Preliminary modeling studies suggest that conformational freedom within the monolayer allows the side chains on at least three and possibly as many as five neighboring  $\beta$ -strands to move close enough to accommodate the 4.14 Å Cd–Cd separation. However, beyond five strands (20 Å), epitaxial growth seems unlikely, whereas it is conceivable that electrostatic interactions between the peripheral carboxylates could stabilize the addition of a few layers of Cd ions to the crystal along the  $\langle 100 \rangle$  direction, yielding the larger crystals observed

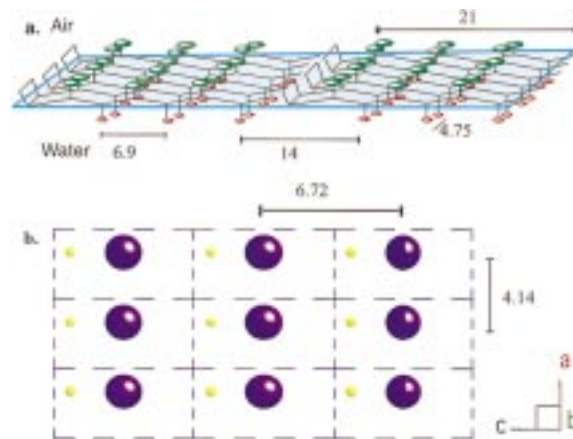


**Figure 4.** (a) Model of the 2D  $\beta$ -sheet assembly of peptidomimetic **A** or **B** at the air–water interface. Hydrophilic groups (Glu or Lys) are represented in red, hydrophobic groups in green. The rectangles represent residue **1**, and the zigzag lines in black denote the polypeptide backbone.  $\beta$ -Sheet formation is stabilized both by intra- and intermolecular hydrogen bonding, whereas, the head-to-tail assembly is presumably mediated by van der Waals forces. The  $\beta$ -strand separation and the alternating  $\text{C}_\alpha$ – $\text{C}_\alpha$  distances are indicated. (b) The cadmium cation (purple) and sulfur anion (yellow) arrangements in the  $\{01.0\}$  plane of CdS (sizes not to scale) in the wurtzite structure.

( $\sim 50$  Å). This may also be the means by which crystals elongate in the  $c$  dimension.

Blue shifts in the UV–vis absorption threshold indicate a decrease in CdS particle size (increased band gap), resulting from the quantum size effect.<sup>10</sup> The absorption threshold for CdS particles nucleated on peptidomimetic (**A**) is 495 nm (2.5 eV band gap vs 2.4 for bulk CdS), whereas CdS particles nucleated on peptidomimetic **B** and CdS crystals grown on an aqueous surface exhibit edge transitions at 530 and 510 nm, consistent with their larger sizes.

In summary, an easily synthesized peptidomimetic assembles into a 2D monolayer at an air–water interface and nucleates the formation of CdS nanocrystallites via the  $\{01.0\}$  face. The degree of lattice matching appears to play a major role in controlling the face nucleated and the crystallite size.

**Acknowledgment.** We thank the NIH R01GM51105, the Skaggs Institute of Chemical Biology, and the Lita Annenberg Hazen Foundation for funding. We thank Kavanagh (UCSD), Addadi (The Weizmann Institute) and Ratnaswamy (Scripps) for suggestions, and Janshof (Scripps) for AFM analysis.

**Supporting Information Available:** UV spectra, AFM image, and bar graph of CdS particle size distribution on peptidomimetic **A** by HR-TEM (PDF). This material is available free of charge via the Internet at <http://pubs.acs.org>.

(10) (a) Fendler, J. H. *Chem. Rev.* **1987**, *87*, 877–899. (b) Henglein, A. *Chem. Rev.* **1989**, *89*, 1861–1873.